

Local Polymer and Solvent Dynamics in Aroclor Solutions: Implications for Solvent Modification

Daniel J. Gisser and M. D. Ediger*

Department of Chemistry, University of Wisconsin, Madison, Wisconsin 53706

Received July 12, 1991; Revised Manuscript Received September 25, 1991

ABSTRACT: The high-frequency limiting viscosity of polybutadiene/Aroclor 1248 solutions is known to be less than that of neat Aroclor. This effect has been attributed to polymer-induced modifications of solvent relaxation. We have performed ^{13}C NMR relaxation experiments to examine simultaneously the rotational dynamics of both components of these solutions. Local segmental motions of polybutadiene are more rapid than solvent rotation. This is unlike the behavior in low-viscosity solvents. With decreasing temperature, solvent rotation slows much more dramatically than do polybutadiene dynamics. Polyisoprene/Aroclor solutions show similar behavior. Polystyrene local dynamics in Aroclor are slower than Aroclor reorientations and have a stronger temperature dependence. The relative time scales for polymer and solvent motion are shown to be an important factor in interpreting solvent modification studies from other laboratories.

Introduction

Internal motions of flexible polymers are often treated through the bead-spring model. This model allows calculation of the spectrum of normal modes and their corresponding relaxation times, τ_k . The solvent generally is viewed as a structureless bath in which the polymer chains freely undergo various Brownian motions. The only important physical property of the solvent is its viscosity, which slows polymer motions. The loss component of the dynamic solution viscosity, η' , is usually assumed to be the sum of the pure solvent's viscosity and a simple contribution from each normal mode. At very high oscillatory driving frequencies, when $\omega\tau_k \gg 1$ for all k , the polymer contribution to η' vanishes, leaving only the solvent contribution.¹

Treatment of the solvent provides a basic difficulty in the interpretation of dynamic mechanical measurements from dilute polymer solutions. These experiments generally find that the high-frequency limiting solution viscosity, η_∞' , is not equal to the pure solvent viscosity, η_s . This observation is inconsistent with the bead-spring model. Attempts to explain this apparent "solvent modification" include a variety of additions to the bead-spring model. Several mechanisms by which η_∞' can be greater than η_s have been proposed, although none are entirely satisfactory. Furthermore, $\eta_\infty' < \eta_s$ for polyisoprene and polybutadiene in Aroclor 1248. Several approaches to these problems have been discussed.²⁻⁹

These dynamic mechanical results have stimulated experimental efforts aimed at studying the solvent directly. Morris, Amelar, and Lodge employed oscillatory electric birefringence to monitor solvent rotational dynamics in polystyrene and polybutadiene solutions in Aroclor.⁶ They found that the solvent relaxation time depends strongly on polymer concentration, lengthening when polystyrene is added but shortening when polybutadiene is added. The changes are strongly temperature dependent in polybutadiene solutions but nearly independent of temperature in polystyrene solutions. Results from polyisoprene/Aroclor solutions are similar to those from polybutadiene/Aroclor, although the effects are smaller.⁷ Other workers have employed other techniques to examine solvent dynamics in these solutions.¹⁰⁻¹²

The concentration dependence of the solvent relaxation time is characterized by an intrinsic effective solvent

viscosity, $[\eta_e]$. $[\eta_e]$ is strongly correlated with $[\eta_\infty']$, the intrinsic value of η_∞' .⁷ This suggests that discrepancies between η_∞' and η_s are mainly caused by modifications to the solvent dynamics by the presence of a polymer. However, the mechanism of this modification is not yet understood on a fundamental level.^{5,7,8}

In the course of seemingly unrelated work^{13,14} we found two surprising and perhaps relevant aspects of polymer solution dynamics: (i) the damping of local polymer dynamics by the solvent can be much less than expected from the macroscopic solvent viscosity; and (ii) local polymer dynamics are faster than the rotation of Aroclor in polyisoprene/Aroclor solutions. Both of these findings are at odds with traditional views of polymer solution dynamics. How can the solvent be considered a *viscous* continuum if the solvent molecules are moving more slowly than the polymer?

This paper is a more detailed and direct exploration of these issues and their relevance to solvent modification. We apply ^{13}C nuclear magnetic resonance relaxation experiments to the problem of solvent modification. This technique allows us to probe Aroclor and polymer dynamics simultaneously. Furthermore, we learn about polymer motions on approximately the length scale of an Aroclor molecule. With these experiments we can explore the relative time scales for polymer and solvent motions on a length scale appropriate for solvent modification. The new data presented here are exclusively from polybutadiene/Aroclor solutions, but we consider polyisoprene and polystyrene/Aroclor solutions as well.

Our results demonstrate that the relative time scales for solvent and local polymer dynamics are fundamentally related to modifications of the solvent viscosity in polymer/Aroclor solutions. This conclusion is valid for solutions of three polymers (polybutadiene, polyisoprene, and polystyrene) in Aroclor. The time scale difference accounts for the direction of the modification of the Aroclor relaxation time (the sign of $[\eta_e]$), its relative magnitude in solutions of the different polymers, and its temperature dependence.

The next three sections of this paper are a complicated and detailed analysis of ^{13}C NMR spin-lattice relaxation data. Readers whose main interest is solvent modification may go directly to the Discussion section. That section contains a summary of our analysis of the polymers' and solvent's dynamics followed by an interpretation of these

* Author to whom all correspondence should be addressed.

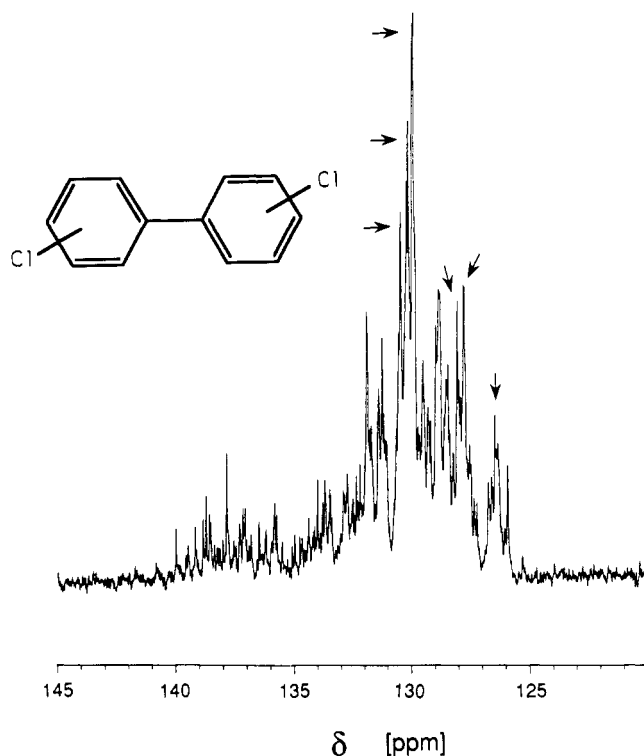


Figure 1. ^1H -Decoupled ^{13}C NMR spectrum of neat Aroclor 1248 (90.6 MHz, 328 K). Peaks at $\delta < 130.5$ ppm are assigned to carbon atoms with directly bonded hydrogens. Arrows indicate peaks included in T_1 calculations. The inset is a generalized structure of an Aroclor molecule. The average molecule has 3.9 Cl atoms.

results within the context of other solvent modification studies.

Experimental Section

Materials and Instrumentation. We have measured natural-abundance, proton-decoupled, ^{13}C spin-lattice relaxation times in solutions of polybutadiene (PB) and polyisoprene (PI) in Aroclor 1248. The Aroclor was a gift from Professor John Schrag and had previously been filtered by his students. This Aroclor (Monsanto Chemical Co., Lot No. KM502) is the same lot as has been used in other solvent modification studies.^{2-4,6} Aroclor is a highly viscous mixture of randomly chlorinated biphenyls (see inset to Figure 1). The exact composition is unknown but contains 48% chlorine by weight (on average, 3.9 chlorine atoms/molecule).

The viscosity of Aroclor 1248 is^{2,13,15}

$$\log \eta = \log (219.0) - \frac{3.0245(T - 298.15)}{T - 242.94 + 6.310 \times 10^{-3}(T - 298.15)^2} \quad (1)$$

for $263 \text{ K} \leq T \leq 318 \text{ K}$ and

$$\log \eta = -0.5482 - \frac{153.73}{244.27 - T} \quad (2)$$

for $277 \text{ K} \leq T \leq 380 \text{ K}$. Equations 1 and 2 give η in centipoise for T in kelvin. Equation 2 is a fit to data found in the literature.¹⁵ The numerical parameters differ slightly from those in ref 13 due to the different temperature ranges considered. We use eq 1 for $T \leq 293 \text{ K}$ and eq 2 for $T > 293 \text{ K}$.

Polybutadiene and polyisoprene were purchased from Good-year. All polymers contained small amounts of antioxidant. Polymer characterization data are given in Table I. Polybutadiene solutions were prepared gravimetrically to 0.0, 1.0, 10, and 20% polybutadiene (w/w). For some calculations we convert concentration units to grams per milliliter, assuming additivity of volumes and densities of 1.45 g/mL for Aroclor and 0.985 g/mL for polybutadiene. Solutions were filtered (0.45 μm) before dissolved oxygen was removed through several freeze-pump-thaw cycles. Samples were sealed under vacuum. The polyisoprene measurements have been reported earlier.¹³

Table I
Polymer Characterization

polymer	polybutadiene	polyisoprene
M_w	24 000	10 200
M_w/M_n	1.1	1.11
% cis-1,4	40	76
% trans-1,4	52	18
% vinyl-1,2	8	0
% vinyl-3,4		6

Spin-lattice relaxation times (T_1) were measured under conditions of complete proton decoupling. Experiments were performed at ^{13}C Larmor frequencies $\omega_C/2\pi = 90.6$ and 25.2 MHz using Bruker AM-360 and AC-100 spectrometers, respectively. A (π - t - $\pi/2$ -FID) pulse sequence¹⁶ was employed, typically with 12–15 delay times t , waiting at least 8 times the longest T_1 of interest between acquisitions. Sample temperature was precise within 1 K and accurate within 2 K. T_1 s generally were reproducible within 5%. Further experimental details are found in refs 13 and 14.

Spectroscopy. The ^1H -decoupled ^{13}C NMR spectrum (90.6 MHz, $T = 328 \text{ K}$) of neat Aroclor is shown in Figure 1. The spectrum is complicated. Each chemically distinct ^{13}C nucleus of each congener of Aroclor gives rise to one peak, many of which overlap. All of these resonances appear within a rather narrow band of the ^{13}C NMR spectral range. The individual NMR peaks broaden dramatically with decreasing temperature, and resolution increases linearly with Larmor frequency. At lower temperatures and lower Larmor frequency the fine structure seen in Figure 1 collapses into a nearly featureless blob.

We wish to learn about solvent rotational dynamics from ^{13}C T_1 data. This is tractable only for the protonated carbons, so some spectral assignment is necessary. Assignment of all the spectral peaks in Figure 1 would be difficult and unnecessary. Fortunately the spectrum is cleanly separable into a protonated ^{13}C region ($\delta < 130.5$ ppm) and a chlorinated and quaternary ^{13}C region ($\delta > 130.5$ ppm). These features strongly support this partial assignment: (i) ^{13}C NMR spectra of some molecularly pure components of Aroclor are assignable and similarly separable.¹⁷ (ii) Peaks at $\delta > 130.5$ ppm have T_1 s an order of magnitude or more longer than peaks at $\delta < 130.5$ ppm. (iii) At high temperatures peak intensities at $\delta < 130.5$ ppm are enhanced by the nuclear Overhauser effect (NOE). Peaks at $\delta > 130.5$ ppm receive a significantly smaller enhancement. Points ii and iii are consistent with the expectation that dipole-dipole relaxation with the bonded proton is efficient for the protonated ^{13}C atoms, which therefore have short T_1 s and benefit from the NOE. The chlorinated and quaternary carbons do not have an efficient spin relaxation mechanism available and therefore have long T_1 s. As these carbons do not relax primarily through ^{13}C - ^1H dipole-dipole exchange, they do not receive a large NOE. The dominant spin relaxation mechanism is unknown for the chlorinated and quaternary carbons, so we have measured and analyzed T_1 from protonated carbons only.

The solvent spin-lattice relaxation times (T_1) we report are averages of T_1 of six of the strongest protonated ^{13}C peaks. These peaks are labeled with arrows in Figure 1. At lower temperatures and/or Larmor frequency, when these peaks are not individually resolved, an appropriately weighted average of the resolved peaks is used to calculate T_1 . As the rotational dynamics of each species present in Aroclor may be different and as different sites on any individual molecule may undergo different dynamics, the various protonated ^{13}C spectral lines may be expected to have different T_1 s. In fact, small but systematic differences were observed in the individual T_1 s. Since the spread in T_1 values was small for any individual experiment (about 20%), we use T_1 to characterize solvent spin-lattice relaxation and molecular reorientation. The complexity of the ^{13}C spectrum precludes definitive distinctions between ortho, meta, and para sites in Aroclor molecules. Spins in para sites might have slightly different T_1 s from spins in ortho and meta sites due to internal rotations about the central C-C biphenyl bond.

The ^{13}C NMR spectrum of polybutadiene is simpler and well understood.¹⁸ Spin-lattice relaxation times are reported and analyzed only for methylene groups in cis and trans repeat units

($\delta = 27$ and 32 ppm, respectively. T_1 data from vinyl-1,2 repeat units are not analyzed due to the low vinyl content of this polymer. The methine carbons appear at 129.0 (cis) and 129.6 ppm (trans), in that part of the spectrum occupied by the protonated carbons of Aroclor. For a 10% (w/w) solution of polybutadiene in Aroclor, the intensities of the polymer methine and solvent peaks are approximately equal. Therefore, it was impossible to calculate T_1 reliably for the methine polybutadiene peaks. The peaks included in the calculations of T_1 for the solvent were chosen to avoid spectral overlap with the polybutadiene methine peaks.

The polyisoprene spectrum presents fewer problems. Following the nomenclature of refs 13 and 14, T_1 data from the methylene carbons C4 ($\delta = 26$ ppm) are analyzed from cis repeat units. Data from carbons C1 and C2 are very similar. The small systematic differences between the various carbons do not affect any of the arguments presented here.

Relaxation Equations. The dominant spin relaxation mechanism in these experiments is a dipole-dipole interaction between ^{13}C and its directly bonded proton(s). Under these conditions T_1 is related to the spectral density function $J(\omega)^{19}$

$$\frac{1}{T_1^{\text{dd}}} = Kn[J(\omega_{\text{H}} - \omega_{\text{C}}) + 3J(\omega_{\text{C}}) + 6J(\omega_{\text{H}} + \omega_{\text{C}})] \quad (3)$$

where ω_{C} and ω_{H} are the ^{13}C and ^1H resonance frequencies and n is the number of bonded protons. The constant K is related to the C-H bond length and taken to be equal to $2.29 \times 10^9 \text{ s}^{-2}$ for methylene carbons and $2.42 \times 10^9 \text{ s}^{-2}$ for methine carbons.¹⁴ $J(\omega)$ is related to the correlation function describing rotational motion of the C-H bond

$$J(\omega) = \frac{1}{2} \int_{-\infty}^{+\infty} \text{CF}(t) e^{i\omega t} dt \quad (4)$$

Thus, T_1 provides information about the average reorientation of a ^{13}C - ^1H bond. By analogy with polyisoprene in dilute solutions,¹⁴ we assume that relaxation with nonbonded protons does not contribute significantly to the polybutadiene T_1 s we report. We also assume nonbonded protons do not contribute significantly to Aroclor T_1 s.

Chemical shift anisotropy (CSA) can contribute to spin relaxation. This effect is insignificant for the methylene carbons of polybutadiene and polyisoprene but is not negligible (7–15%) for Aroclor at the higher Larmor frequency used. The spin-lattice relaxation rate is a sum of the dipole-dipole and CSA relaxation rates¹⁹

$$\frac{1}{T_1} = \frac{1}{T_1^{\text{dd}}} + \frac{1}{T_1^{\text{CSA}}} \quad (5)$$

where T_1^{dd} is the dipole-dipole contribution from eq 3. If the chemical shift is axially symmetric, T_1^{CSA} is given by¹⁹

$$\frac{1}{T_1^{\text{CSA}}} = \frac{2}{15} \omega_{\text{C}}^2 (\sigma_{\parallel} - \sigma_{\perp})^2 J(\omega_{\text{C}}) \quad (6)$$

Although use of eq 6 is an approximation,¹⁴ it should be adequate since CSA provides only a minor contribution to T_1 . We have assumed $(\sigma_{\parallel} - \sigma_{\perp}) = 200$ ppm for Aroclor and $(\sigma_{\parallel} - \sigma_{\perp}) = 0$ ppm for polybutadiene.²⁰

Aroclor Dynamics

Neat Aroclor. Spin-lattice relaxation times of neat Aroclor have been measured at two Larmor frequencies over the temperature range 276–363 K. The data are plotted in an Arrhenius-like format in Figure 2. T_1 minima are seen in both data sets, and an ω_{C} -independent, extreme narrowing regime seems to appear at high temperatures. We will show that (i) a distribution of time constants is required to describe Aroclor rotation, (ii) the shape of this distribution does not change over the temperature range studied, (iii) the temperature dependence of Aroclor rotation follows the Stokes-Einstein-Debye prediction, and (iv) this temperature dependence is in excellent agreement with measurements performed at higher and lower temperature ranges with two other techniques.

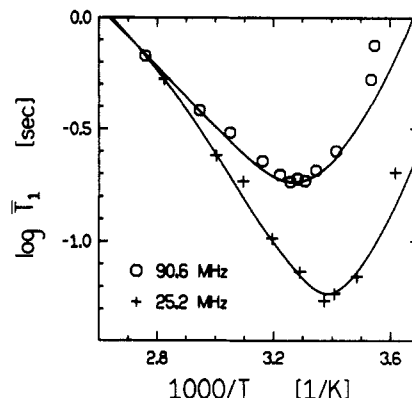


Figure 2. Spin-lattice relaxation data (T_1) of neat Aroclor as a function of temperature and Larmor frequency. Experimental uncertainty ($\pm 5\%$) is given by the size of the data points. The solid curves are a fit to the Cole-Davidson model with $\gamma = 0.30$ and $B = 13\,200 \text{ (ps}\cdot\text{K)/cP}$.

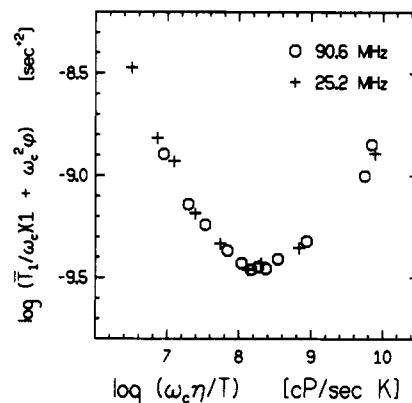


Figure 3. Frequency-temperature superposition of T_1 data from neat Aroclor. The data are from Figure 2. See text for an explanation of the axes. This superposition confirms $\tau_{\text{Aro}} \propto \eta/T$ and demonstrates that the distribution of motional time constants has a shape independent of temperature.

The two data sets shown in Figure 2 can be superposed by a Larmor frequency-temperature superposition. This approach was introduced in the analysis of bulk polybutadiene²¹ and has also been employed in the analysis of local polyisoprene dynamics in dilute solution.¹⁴ The superposition for neat Aroclor T_1 s is shown in Figure 3. In ref 14 the vertical axis is $\log (T_1/\omega_{\text{C}})$. Here a small correction term $(1 + \omega_{\text{C}}^2 \phi)$ has been incorporated to account for CSA relaxation. ϕ represents the ratio²² $T_1^{\text{dd}}/\omega_{\text{C}}^2 T_1^{\text{CSA}}$ and is approximated as $\phi = (\sigma_{\parallel} - \sigma_{\perp})^2/75nK = 2.5 \times 10^{-19} \text{ s}^2$. Following refs 21 and 14, the horizontal axis should be $\log (\omega_{\text{C}} \tau_{\text{Aro}})$, where τ_{Aro} is a time constant characterizing Aroclor rotation. We have instead plotted $\log (\omega_{\text{C}} \eta/T)$ on the horizontal axis, as $\tau_{\text{Aro}} \propto \eta/T$ if the Stokes-Einstein-Debye relationship holds.

The superposition shown in Figure 3 is excellent, confirming that Aroclor rotation does follow the Stokes-Einstein-Debye law over the experimental temperature range. The superposition also demonstrates that the distribution of time constants needed to describe Aroclor rotation does not appreciably change shape with temperature.

A single rotational time constant (equivalently, an exponential correlation function) is inconsistent with the NMR data. The values of T_1 at the T_1 minima most readily demonstrate this. An exponential CF(t) predicts that, at the minima, $T_1 = 0.11$ and 0.035 s at $\omega_{\text{C}}/2\pi = 90.6$ and 25.2 MHz , respectively. The experimental values of T_1 are about 60% longer. Of course, the necessity of using an

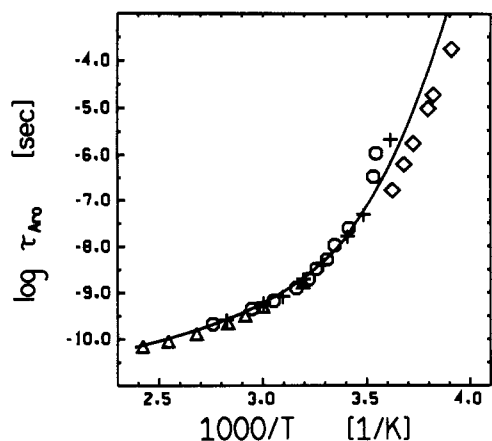


Figure 4. Arrhenius plot of the molecular reorientation time of Aroclor calculated from three techniques: DRS (Δ); ^{13}C NMR T_1 (O, 90.6 MHz) and (+, 25.2 MHz); and OEB (\diamond). The curve is $B\eta/T$ with $B = 13\,200$ (ps·K)/cP.

average \bar{T}_1 for Aroclor also indicates that an exponential CF(t) is insufficient. This conclusion is somewhat at odds with depolarized Rayleigh scattering (DRS) studies of neat Aroclor rotation. At temperatures above those used in this study, DRS experiments suggest that an exponential CF(t) is sufficient.¹¹ At temperatures below those used in this study, however, oscillatory electric birefringence (OEB) experiments indicate the presence of a distribution of relaxation times.⁶

In addition to the exponential model, we have attempted to fit the Aroclor \bar{T}_1 data with a biexponential CF(t), as well as Cole–Cole,^{23,24} Fuoss–Kirkwood,^{23,25} $\log \chi^2$,^{23,26} rectangular,²⁷ and Cole–Davidson^{27,28} distributions of time constants. The fitting procedure has been described earlier.¹⁴ We have constrained

$$\tau = B[\eta(T)]/T \quad (7)$$

for all τ in the distributions of time constants, $F(\tau)$. This constraint comes from the success of the \bar{T}_1 superposition in Figure 3. Only the Cole–Davidson distribution provides a satisfactory fit.

The Cole–Davidson spectral density function is given by²⁷

$$J(\omega) = \frac{\sin[\gamma \tan^{-1}(\omega \tau_{\max})]}{\omega(1 + \omega^2 \tau_{\max}^2)^{\gamma/2}} \quad (8)$$

The best fit of this model to the Aroclor \bar{T}_1 data has $\gamma = 0.30$ and $B = 13\,200$ (ps·K)/cP, when τ_{\max} is used in place of τ in eq 7. This fit has a reduced χ_r^2 of 1.8 and is shown as the solid curves in Figure 2. It is not our purpose to determine conclusively the correct $J(\omega)$ for neat Aroclor. However, we do require a reasonable fit so that we may analyze the concentration dependence of the solvent \bar{T}_1 in polybutadiene/Aroclor solutions. The Cole–Davidson distribution has a singularity at the longest time constant (τ_{\max}) and a decaying distribution of shorter time constants. This shape is roughly consistent with OEB data, which are “highly suggestive of the appearance of additional relaxation processes at much higher frequencies”.⁶

The time constant τ_{Aro} describing neat Aroclor rotation is plotted in an Arrhenius format in Figure 4. The NMR points (O, +) are from the Cole–Davidson fit to \bar{T}_1 data, with τ_{Aro} taken equal to τ_{\max} . Results from DRS¹¹ (Δ) and OEB⁶ (\diamond) experiments are also included. The curve is the temperature dependence of η/T of Aroclor 1248, plotted according to eq 7 with $B = 13\,200$ (ps·K)/cP, as calculated above.

For the NMR points in Figure 4, τ_{Aro} cannot be calculated from a single value of \bar{T}_1 . The entire collection of \bar{T}_1 values, measured at two Larmor frequencies and multiple temperatures, was analyzed as a whole. This analysis led to several conclusions, eq 7 among them. Thus, the NMR results are most accurately depicted as the curve shown in Figure 4. The circles (90.6 MHz) and plus symbols (25.2 MHz) in Figure 4 represent calculations of τ_{\max} from \bar{T}_1 , assuming a Cole–Davidson spectral density function with $\gamma = 0.30$ and $B = 13\,200$ (ps·K)/cP.

Although the proportionality constants are not certain, the temperature dependence of τ_{Aro} follows η/T for each technique. The three experimental techniques agree quite well, particularly considering several ambiguities in the comparisons.

Several possible explanations can account for the differences in absolute values of τ_{Aro} from OEB and NMR over the intersecting temperature range. The values of τ_{Aro} depend on details of the data analysis. One reasonable alternate analysis of the raw OEB data leads to τ_{Aro} s a factor of ~ 4 longer without greatly affecting the temperature dependence.⁶ Similarly, if τ_{Aro} (from NMR) was defined as the time integral of CF(t) rather than as τ_{\max} , the values of τ_{Aro} would be approximately $1/3$ of those plotted in Figure 4. Either of these uncertainties would substantially bring the OEB and NMR results into agreement. The discrepancies between the experiments could also be real, not simply artifacts of the analyses. The three experiments monitor rotations of different vectors and preferentially monitor different molecules of the Aroclor mixture. NMR, for example, is more sensitive to Aroclor molecules with more hydrogens and fewer chlorines. If chemically different Aroclor molecules rotate differently, exact determinations of τ_{Aro} from different techniques would not be expected to agree.²⁹

Aroclor Dynamics in Polybutadiene Solutions. In this section we calculate reorientation times, $\tau_{\text{Aro}}(c, T)$, of Aroclor as a function of temperature and polybutadiene concentration. These times will be used to calculate

$$\zeta(c, T) \equiv \frac{\tau_{\text{Aro}}(c, T)}{\tau_{\text{Aro}}(c=0, T)} \equiv \frac{\tau_{\text{Aro}}(c, T)}{\tau_{\text{Aro}}} \quad (9)$$

$\zeta(c, T)$ characterizes the change in solvent dynamics upon addition of polymer and presumably is related to changes in local friction. Other workers have found that $\zeta(c, T)$ is an exponential function of concentration:^{6,7,10–12}

$$\zeta(c, T) \equiv \frac{\tau_{\text{Aro}}(c, T)}{\tau_{\text{Aro}}} = e^{[\eta_a]c} \quad (10)$$

Our $\partial \ln \zeta(c, T) / \partial c$ results for polybutadiene/Aroclor solutions are consistent with results from other techniques. The NMR results presented here also clarify the extent of solvent modification at temperatures above those studied with the OEB experiments.

Spin–lattice relaxation times of Aroclor in polybutadiene/Aroclor solutions have been measured at 90.6 MHz. Figure 5 shows \bar{T}_1 of the solvent as a function of temperature and polymer concentration. \bar{T}_1 is only a weak function of polymer concentration, indicating that solvent dynamics are not strongly modified by the presence of the polymer over this temperature range. The small changes in \bar{T}_1 are significant, however. The \bar{T}_1 minimum shifts to lower temperatures as polybutadiene is added, indicating that Aroclor rotation becomes faster in more concentrated solutions. The \bar{T}_1 minimum also shifts to longer \bar{T}_1 s upon addition of polybutadiene, suggesting that the distribution of time constants describing Aroclor rotation broadens

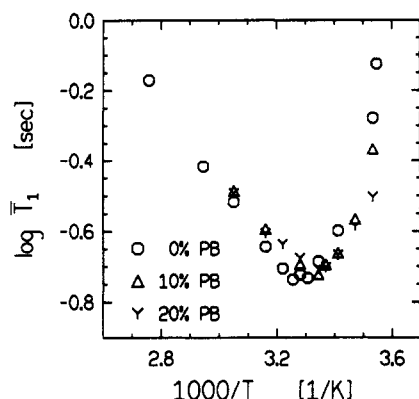


Figure 5. Aroclor T_1 data (90.6 MHz) from polybutadiene/Aroclor solutions plotted in an Arrhenius-like format. The symbols represent different polybutadiene concentrations. The T_1 minimum shifts to slightly lower temperature and longer T_1 in the more concentrated solutions.

slightly in more concentrated solutions. This second feature introduces some ambiguity into the following analysis. We use two different approaches to calculate $\zeta(c, T)$.

Method I assumes that the Cole-Davidson distribution remains an adequate description of Aroclor dynamics in polybutadiene/Aroclor solutions and that only the width parameter γ needs to be adjusted. γ is determined solely by the value of T_1 at the minimum: $\gamma = 0.30, 0.30, 0.28$, and 0.27 for $0, 1, 10$, and 20% polybutadiene solutions, respectively. Each T_1 value then determines τ_{\max} for the given concentration and temperature. $\zeta(c, T)$ is then calculated as $\tau_{\max}(c, T)/\tau_{\max}(c=0, T)$.

Method II neglects the slight variation in the functional form of $J(\omega)$ with concentration. This assumption allows calculation of $\zeta(c, T)$ without invoking any specific motional model. Each $\log T_1$ versus $1000/T$ curve was vertically shifted so that at the minimum $T_1 = 0.184$ s, the value for neat Aroclor. (The 1% solution data did not require this shift.) We have already shown in a model independent manner that τ_{Aro} scales as η_{Aro}/T . This result, together with the assumption that $\tau_{\text{Aro}} = 2$ ns at the T_1 minimum, allows a mapping from T_1 to τ_{Aro} for neat Aroclor. We use this same mapping for the T_1 measurements of Aroclor in solution with polybutadiene to obtain $\tau_{\text{Aro}}(c, T)$. Since $\zeta(c, T)$ is formed from the ratio $\tau_{\text{Aro}}(c, T)/\tau_{\text{Aro}}(0, T)$, the assumption about the absolute value of τ_{Aro} at the T_1 minimum is not actually necessary.

Our $\zeta(c, T)$ results can neither confirm nor deny that $\zeta(c, T)$ is an exponential function of concentration. We assume this functional form and calculate $\partial \ln \zeta(c, T)/\partial c$ at each experimental temperature from the slope of $\ln \zeta(c, T)$ vs c . An example is shown as an inset to Figure 6.

Table II lists the values of $\partial \ln \zeta(c, T)/\partial c$ calculated from the two analyses of the temperature and concentration dependence of T_1 . Quite different assumptions went into the two analyses. Method I acknowledges a concentration dependence in $J(\omega)$. We assume that the Cole-Davidson distribution function, with different values of γ , provides $J(\omega)$ for the different solutions. Method II does not invoke a particular motional model but overlooks the concentration dependence in $J(\omega)$. The two methods lead to similar values of $\partial \ln \zeta(c, T)/\partial c$. This consistency lends credence to the results.

A comparison of our measurements of Aroclor dynamics with results from other techniques is shown in Figure 6. The vertical axis is the quantity calculated in the preceding paragraphs and represents the modification of solvent dynamics upon addition of polymer. When $\partial \ln \zeta(c, T)/\partial c$

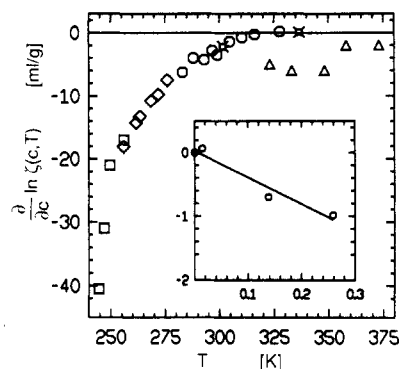


Figure 6. Temperature dependence of the modification of Aroclor dynamics in polybutadiene/Aroclor. The large negative values of $\partial \ln \zeta(c, T)/\partial c$ indicate solvent motions become much more rapid as polybutadiene is added to the solutions. Data from five techniques are included: PCS (\square); OEB (\diamond); ^{13}C NMR T_1 (\circ); PFG-NMR (small squares with exterior diagonals); and DRS (Δ). PFG-NMR reflects translational motion of solvent molecules; all others reflect rotational motion. The inset is an example plot (method II; 288 K) of $\ln \zeta(c, T)$ versus c [g/mL]. The best fit line has slope $\partial \ln \zeta(c, T)/\partial c = -4.2$ mL/g.

Table II
 $\partial \ln \zeta(c, T)/\partial c$ (mL/g) Obtained from Aroclor T_1 Data

temp, K	method I	method II
328	+0.2	+0.2
316	-0.1	-0.4
311	-0.7	-0.7
305	-1.6	-1.2
299	-4.6	-2.5
297	-2.8	-2.8
293	-4.2	-4.4
288	-3.8	-4.2
283	-6.7	-6.0

$= 0$, solvent dynamics are independent of polymer concentration. When $\partial \ln \zeta(c, T)/\partial c < 0$, Aroclor motions are faster in polymer solutions than in neat Aroclor, and when $\partial \ln \zeta(c, T)/\partial c > 0$, solvent motions are slower in polymer solutions. The circles in Figure 6 are the ^{13}C NMR T_1 results of this work. Averages from the two analyses in Table II are plotted. Other workers have employed photon correlation spectroscopy¹² (PCS; \square), oscillatory electric birefringence⁶ (OEB; \diamond), and depolarized Rayleigh scattering¹² (DRS; Δ) to study solvent rotation in polybutadiene/Aroclor solutions. These results are included in Figure 6. Two points reflecting the modification of translational solvent diffusion were obtained by pulsed field gradient nuclear magnetic resonance¹⁰ (PFG-NMR; small squares with exterior diagonals).

Several features of Figure 6 are noteworthy. Most important, results from five techniques generally follow a single curve. We are unsure why the DRS results deviate from the ^{13}C NMR T_1 and PFG-NMR results. At low temperatures the presence of polybutadiene dramatically enhances solvent mobility. At higher temperatures this effect becomes much smaller. Apparently $\partial \ln \zeta(c, T)/\partial c$ is asymptotically approaching zero or some other small value at high T . In addition, rotational and translational diffusion of Aroclor seem to be similarly affected by the presence of polybutadiene, as demonstrated by the agreement between the PFG-NMR and ^{13}C NMR T_1 results.

Local Polymer Dynamics

^{13}C NMR T_1 data of polymers in dilute solutions are related to motions of C-H bonds in the polymer chain. The measurements reported and analyzed in this paper

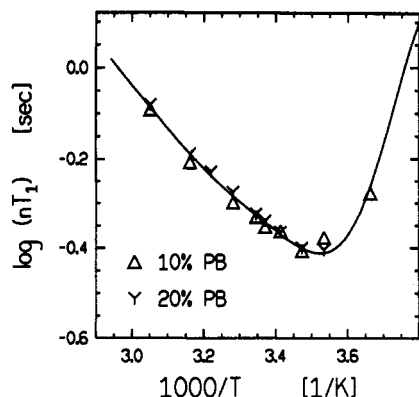


Figure 7. Spin-lattice relaxation times (90.6 MHz) of polybutadiene in Aroclor solutions plotted in an Arrhenius format. Data are from methylene carbons ($n = 2$) in trans repeat units. T_1 s from two concentrations are shown. The curve is a fit of a biexponential correlation function to the data. Reasonable fits require $\alpha \approx 0.3$ and $E_a \approx 11$ kJ/mol.

reflect reorientations of some short sections of the polymer backbones. For polybutadiene and polyisoprene this length scale is believed to be 1–2 repeat units.

Polyisoprene in Aroclor Solutions. The local dynamics of polyisoprene in dilute solutions are already understood in considerable detail.^{13,14,30,31} The forms of the correlation functions describing local segmental dynamics are nearly independent of temperature and solvent. A biexponential correlation function describes local polyisoprene dynamics in toluene quite well.¹⁴ That is

$$CF(t) = (1 - f)e^{-t/\tau_{\text{seg}}} + fe^{-t/\tau_{\text{lib}}} \quad (11)$$

with $0 < f < 1$ and $\tau_{\text{seg}} > \tau_{\text{lib}}$. The time constant τ_{seg} reflects activated transitions between conformational potential energy minima. These motions occur on the length scale of 1–2 repeat units, approximately the size of a solvent molecule. Librations of only a few atoms appear through τ_{lib} . Most important, in toluene, Aroclor, and eight other solvents, the temperature dependence of τ_{seg} is

$$\tau_{\text{seg}} = A\eta^\alpha e^{E_a/RT} \quad (12)$$

A , α , and E_a are properties of the polymer only. $A = 0.39$ ps/cP $^\alpha$, $\alpha = 0.41$, and $E_a = 13$ kJ/mol. The temperature dependence of τ_{lib} is unknown and has little effect on the interpretation of ^{13}C NMR T_1 data. Probably τ_{lib} is nearly independent of solvent, viscosity, and temperature. For polyisoprene in toluene, $\tau_{\text{seg}}/\tau_{\text{lib}} \geq 500$ at 200 K.

Polybutadiene in Aroclor Solutions. Spin-lattice relaxation times from polybutadiene in Aroclor solutions are plotted in Figure 7. The data are from methylene ^{13}C spins in trans repeat units of the polymer. Data from two polymer concentrations (10 and 20%) are included. T_1 data from cis CH_2 groups (not shown) are qualitatively similar. Due to spectral interference with the solvent, it was impossible to measure T_1 s from cis or trans CH groups of polybutadiene.

Results from the two concentrations agree within experimental uncertainty. This is unlike the Aroclor T_1 data from these same solutions, which are concentration dependent. This discrepancy may be surprising. On the other hand, since NMR reflects very local polymer motions, T_1 s generally are independent of polymer concentration below 15 or 20% polymer. At lower temperatures a concentration dependence could appear in the polymer T_1 s. Since the T_1 s we measure are independent of concentration, we analyze all of the data in Figure 7 together, without regard to concentration.

Not enough data exist to determine unambiguously the form of $CF(t)$ or the temperature dependence of local polybutadiene dynamics in Aroclor. As polyisoprene and polybutadiene are quite similar structurally, we assume that local polybutadiene dynamics are similar to those of polyisoprene. Specifically, we assume that eqs 11 and 12 can describe polybutadiene dynamics in Aroclor.

The curve shown in Figure 7 is a fit of the data to a biexponential $CF(t)$ (eq 11) with the temperature dependence given by eq 12. The fitting routine is described in more detail in ref 14. We have assumed $\tau_{\text{seg}}/\tau_{\text{lib}} = 1000$ at all temperatures. The other fit parameters are expected to be insensitive to the value of $\tau_{\text{seg}}/\tau_{\text{lib}}$ as long as $\tau_{\text{seg}}/\tau_{\text{lib}}$ is greater than about 200.¹⁴ The remaining parameters defining the curve are $\alpha = 0.30$, $E_a = 11$ kJ/mol, $f = 0.66$, and $A = 1.3$ ps/cP $^\alpha$. Although there are too many parameters in this model to evaluate any of them precisely, reasonable values of E_a are obtained only if $\alpha = 0.30 \pm 0.06$. The agreement between the curve and the data is much worse for $\alpha > 0.4$. E_a and α are strongly correlated parameters: for $\alpha > 0.36$, $E_a < 5$ kJ/mol, while for $\alpha < 0.24$, $E_a > 16$ kJ/mol.

Analysis of preliminary polybutadiene ^{13}C T_1 data in five solvents (hexane, tetrahydrofuran, squalene, bis(2-ethylhexyl) phthalate, and Aroclor) gives values of α and E_a consistent with those discussed above. An isothermal plot ($T = 328$ K, $\omega_C/2\pi = 90.6$ MHz) of $\log T_1^{-1}$ vs $\log \eta$, analogous to Figure 6 of ref 13, has slope $\alpha \approx 0.35$. The activation energy (E_a) is about 9 kJ/mol in tetrahydrofuran.

The preceding paragraphs have exclusively discussed polybutadiene CH_2 groups in trans repeat units. In Aroclor, the cis CH_2 data can be fit by $\alpha = 0.32$, $E_a = 11$ kJ/mol, $f = 0.62$, $A = 0.91$ ps/cP $^\alpha$, and $\tau_{\text{seg}}/\tau_{\text{lib}} = 1000$. Reasonable fits require $\alpha = 0.32 \pm 0.06$ for $E_a = 10 \pm 6$ kJ/mol. Experiments in the other solvents suggest $\alpha = 0.37$ and $E_a = 10$ kJ/mol. The cis and trans CH groups could not be studied in Aroclor solutions due to spectral overlap with the solvent, but they have similar values of α and E_a in the four other solvents.

In this section we have used ^{13}C T_1 measurements to show that local polybutadiene dynamics follow the temperature and solvent viscosity dependence of eq 12 with $\alpha \approx 0.3$, $E_a \approx 11$ kJ/mol, and $A \approx 1.3$ ps/cP $^\alpha$. These values were calculated from temperature-dependent T_1 s of polybutadiene trans CH_2 groups in Aroclor. Similar values were obtained for polybutadiene cis CH_2 groups in Aroclor. T_1 data from both CH_2 groups and cis and trans CH groups in four other solvents also lead to comparable values of α and E_a . The overall agreement among these calculations provides reasonable confidence in the resulting parameters.

Polystyrene in Aroclor Solutions. Polystyrene motions in Aroclor probably are too slow to be addressed easily by ^{13}C T_1 measurements. However, we can estimate α and E_a from data in the literature. Data are only available for polystyrene solutions with solvents other than Aroclor, but like polybutadiene (discussed above) and polyisoprene,¹³ we expect α and E_a to be independent of the solvent identity.

At high temperatures and low solvent viscosities, and when experiments are performed at low enough Larmor frequencies (i.e., when $\omega_C\tau_{\text{PS}} \ll 1$), T_1 is inversely proportional to τ_{PS} . Several workers have examined polystyrene ^{13}C T_1 s in dilute solutions. Figure 8 is a plot of T_1^{-1} vs η for the backbone C–H carbon of atactic polystyrene in various solvents at $T = 333$ K and $\omega_C/2\pi \approx 24$ MHz.^{32–34} In some cases it was necessary to interpolate to 333 K. We believe $\omega_C\tau_{\text{PS}} \ll 1$ for this data, so $T_1^{-1} \propto \tau_{\text{PS}}$. Since the data fall approximately on a line

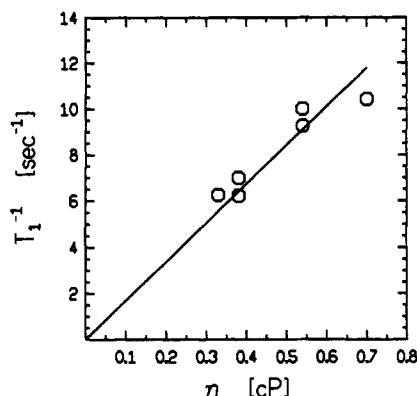


Figure 8. T_1^{-1} vs η for the backbone C-H carbon of atactic polystyrene in various solvents (24 MHz, 333 K). Data are from the literature.³²⁻³⁴ A solid line through the origin provides a reasonable fit to the data. Since $T_1^{-1} \propto \tau_{PS}$, this figure shows that $\tau_{PS} \propto \eta^\alpha$ with $\alpha = 1$.

passing through the origin, the viscosity exponent (from eq 12) α is equal to 1. An analogous plot with similar results has been made for $T = 348$ K.

Other work confirms that local polystyrene dynamics slow linearly with increasing solvent viscosity. Gronski and Murayama³³ have measured atactic polystyrene ^{13}C T_1 s as a function of temperature in two solvents: tetrahydrofuran and cyclohexane. The activation energies E_{exp} obtained from a plot of $\ln T_1$ vs $1000/T$ are different in the two solvents. However, E_{exp} was easily decomposed into a sum of two parts: a contribution of the solvent viscosity (E_η) and an intramolecular potential energy barrier (E_a). $E_a = 20$ kJ/mol in both solvents. This analysis is equivalent to showing $\alpha = 1$. The prefactor A in eq 12 is 0.5 ps/cP. Heatley and Wood³⁵ have argued that Kramers' theory ($\alpha = 1$) also provides an appropriate framework for analyzing ^1H T_1 s of polystyrene solutions. Grandjean et al.³⁶ have presented a similar argument for ^2H T_1 s of deuterated polystyrenes. Finally, in our laboratories, Waldow et al.³⁷ have employed time-resolved fluorescence anisotropy measurements to show that $\alpha = 0.9 \pm 0.05$ for anthracene-labeled polystyrene.

Discussion

In the preceding sections we have analyzed solvent and polymer ^{13}C T_1 data from polybutadiene, polyisoprene, and polystyrene solutions. These data were related to the time scales of solvent rotation and local polymer dynamics. The analysis can be summarized in four equations

$$\tau_{\text{Aro}} = (13\,200(\text{ps}\cdot\text{K})/\text{cP})\eta/T \quad (13)$$

$$\tau_{\text{PS}} = (0.5\text{ ps}/\text{cP})\eta e^{(+20\text{ kJ/mol})/RT} \quad (14)$$

$$\tau_{\text{PI}} = (0.39\text{ ps}/\text{cP}^{0.41})\eta^{0.41} e^{(+13\text{ kJ/mol})/RT} \quad (15)$$

$$\tau_{\text{PB}} = (1.3\text{ ps}/\text{cP}^{0.3})\eta^{0.3} e^{(+11\text{ kJ/mol})/RT} \quad (16)$$

τ_{Aro} is the molecular rotation time for neat Aroclor 1248. The time constants for the three polymers (τ_{poly}) are associated with segmental motions of the chain backbones in dilute solutions in Aroclor. η is the viscosity of neat Aroclor 1248. Equation 13 is derived from data over the temperature range 263–413 K,²⁹ eq 16 from data at 273–328 K, and eq 15 from data at 325–357 K. Equation 14 is an extrapolation from local polystyrene dynamics in other solvents.

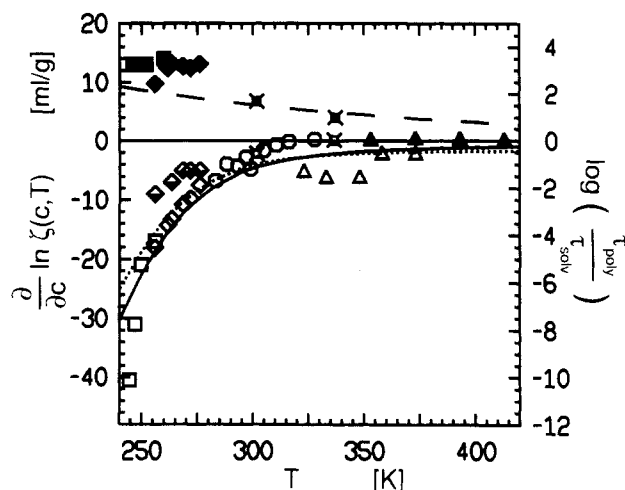


Figure 9. Temperature dependence of the modifications of Aroclor dynamics in polymer/Aroclor solutions (points, left axis) compared to the ratio of time scales for local polymer and solvent dynamics (curves, right axis). Polybutadiene points are from Figure 6. The fully darkened points are for polystyrene solutions, the half-darkened points are for polyisoprene, and the open points are for polybutadiene. Point shapes correspond to different experimental techniques (text contains key and references). The dashed curve is for polystyrene solutions, the dotted curve for polyisoprene, and the full curve for polybutadiene.

We believe that the modifications of Aroclor's dynamics in polymer solutions are related to the polymer chains' dynamics. The pertinent polymer dynamics must be very local, on the length scale of approximately 1 solvent molecule. Equations 13–16 allow calculation of the ratio $\tau_{\text{poly}}/\tau_{\text{Aro}}$ for the three polymer solutions. We might expect that when $\tau_{\text{poly}} > \tau_{\text{Aro}}$, solvent motions would slow upon addition of polymer. Similarly, we anticipate that when $\tau_{\text{poly}} < \tau_{\text{Aro}}$, solvent rotation could speed up as polymer is added. These ideas are consistent, for example, with suggestions from coupling theory.⁹

The fundamental observation of this paper is that the relative time scales for polymer and solvent motions are intimately related to the modification of solvent dynamics upon addition of the polymers. Figure 9 shows the relationships between $\tau_{\text{poly}}/\tau_{\text{Aro}}$ and the polymer concentration dependence of $\tau_{\text{Aro}}(c, T)$. A great deal of information is contained in Figure 9. The points characterize the concentration dependence of $\tau_{\text{Aro}}(c, T)$ for Aroclor 1248 in solutions with polystyrene (darkened symbols), polyisoprene (half-darkened diamonds), or polybutadiene (open symbols). Data from several experimental techniques and researchers are included: PCS¹² (squares), OEB^{6,7} (diamonds), ^{13}C NMR T_1 (circles, this work), DRS^{11,12} (triangles), and PFG-NMR¹⁰ (small squares with exterior diagonals). The points from polybutadiene/Aroclor solutions are reproduced from Figure 6. All these data correspond to the left vertical axis.

The curves in Figure 9 are $\tau_{\text{poly}}/\tau_{\text{Aro}}$ plotted on a logarithmic scale (right vertical axis). They are for solutions of polybutadiene (—), polyisoprene (···), and polystyrene (---) in Aroclor. These curves have been calculated directly from eqs 13–16. The two vertical axes have been aligned with a common zero and have been arbitrarily scaled with respect to one another.

Figure 9 demonstrates the close association between the concentration dependence of $\tau_{\text{Aro}}(c, T)$ and the relative time scales of local polymer and solvent dynamics. All of the qualitative features of the $\partial \ln \zeta(c, T)/\partial c$ data are apparent in the $\log(\tau_{\text{poly}}/\tau_{\text{Aro}})$ curves. For polystyrene, $\partial \ln \zeta(c, T)/\partial c$ and $\log(\tau_{\text{poly}}/\tau_{\text{Aro}})$ are both positive at all

temperatures. When local polymer motions are slower than solvent rotation, solvent rotation slows upon addition of polymer. Similarly, $\partial \ln \zeta(c, T) / \partial c$ and $\log(\tau_{\text{poly}} / \tau_{\text{Aro}})$ are both less than or approximately equal to zero at all temperatures for polybutadiene and polyisoprene solutions. When local polymer motions are faster than solvent rotation, solvent rotation speeds up upon addition of polymer.

In addition to correctly recovering the signs of $\partial \ln \zeta(c, T) / \partial c$, the relative magnitudes are approximately reproduced by $\log(\tau_{\text{poly}} / \tau_{\text{Aro}})$. In the temperature range of the OEB experiments (256–276 K), $\partial \ln \zeta(c, T) / \partial c$ for polystyrene and polybutadiene are about equal in magnitude but opposite in sign. For polyisoprene the effect is similar to polybutadiene but smaller. These trends also are apparent in the $\log(\tau_{\text{poly}} / \tau_{\text{Aro}})$ curves. Thus, the change in the solvent dynamics upon addition of polymer is approximately proportional to the (logarithmic) difference in time scales between the solvent and local polymer dynamics.

The temperature dependence of $\partial \ln \zeta(c, T) / \partial c$ also is emulated by the $\log(\tau_{\text{poly}} / \tau_{\text{Aro}})$ curves. For all three polymers the absolute values of both quantities are largest at low temperatures, but both $\partial \ln \zeta(c, T) / \partial c$ and $\log(\tau_{\text{poly}} / \tau_{\text{Aro}})$ seem to approach zero at higher temperatures. At low T the temperature dependences are quite strong for polybutadiene and polyisoprene but weak for polystyrene solutions. These trends are understood in the context of eqs 13–16; the temperature dependence in these equations predominantly appears in the temperature dependence of the viscosity of Aroclor. In polystyrene/Aroclor, the solvent viscosity precisely cancels out of $\log(\tau_{\text{PS}} / \tau_{\text{Aro}})$. Nearly all of the temperature dependence appears in the Arrhenius term describing local polymer dynamics. As seen in Figure 9, this provides only a modest variation in $\log(\tau_{\text{PS}} / \tau_{\text{Aro}})$. Since local polystyrene dynamics are more strongly temperature dependent than solvent rotation, $\log(\tau_{\text{PS}} / \tau_{\text{Aro}})$ decreases at higher temperatures.

Unlike the above situation with polystyrene/Aroclor, the solvent viscosity does not cancel in $\log(\tau_{\text{PB}} / \tau_{\text{Aro}})$ and $\log(\tau_{\text{PI}} / \tau_{\text{Aro}})$. Aroclor dynamics change much more dramatically with temperature than do polyisoprene or polybutadiene dynamics. This is a result of the nonlinear relationship between τ_{poly} and the solvent viscosity for polybutadiene and polyisoprene. The activation energy terms are less important than the $\eta^{1-\alpha}$ terms which appear in $\tau_{\text{PI}} / \tau_{\text{Aro}}$ and $\tau_{\text{PB}} / \tau_{\text{Aro}}$. The very strong temperature dependence of Aroclor's viscosity leads to the strong temperature dependence of $\log(\tau_{\text{poly}} / \tau_{\text{Aro}})$.

If a linear relationship between the time scales for local polymer dynamics and the solvent viscosity had been assumed, the comparison between $\tau_{\text{poly}} / \tau_{\text{Aro}}$ and $\partial \ln \zeta(c, T) / \partial c$ would have failed completely. A nonlinear relationship between local dynamics and solvent viscosity (in the form of eq 12) was first observed by Glowinkowski and co-workers.¹³ An extensive discussion of this effect has been presented.^{13,31} Kramers' theory, which provides the usual framework for discussing local polymer dynamics, predicts $\alpha = 1$, as is surmised for polystyrene. A power law relationship between τ_{poly} and η , with $0 \leq \alpha \leq 1$, is consistent with the suggestion that the frequency dependence of solvent friction must be considered when conformational changes occur rapidly compared to a time constant characteristic of solvent motions.^{38–41}

Several aspects regarding the curves in Figure 9 merit further comment and study. Most important, the calculations of τ_{poly} from eqs 14–16 have been extrapolated beyond the experimentally accessed temperature ranges. Additionally, the scaling of the two vertical axes in Figure

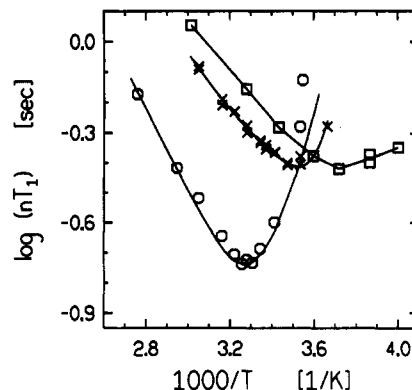


Figure 10. Spin-lattice relaxation times of neat Aroclor (O), bulk polybutadiene (\square), and dilute polybutadiene in Aroclor (\times). The curves through the neat Aroclor and polybutadiene solution data are reproduced from Figures 2 and 7. The bulk polybutadiene data are from ref 21 and are connected by line segments. The data show that local motions of Aroclor are slower than those of polybutadiene and that local polybutadiene motions are slower in Aroclor solutions than in the undiluted polymer.

9 is arbitrary. The decision to align the two zeroes seems reasonable: if $\tau_{\text{poly}} = \tau_{\text{Aro}}$, then τ_{Aro} is not expected to depend on polymer concentration. The fact that the same vertical scaling factor applies for all three polymers is encouraging, although justification for doing otherwise could easily be found: the detailed motions of the different materials are different, so the absolute values of the time constants are not precisely comparable.

Some of the conclusions from Figure 9 can also be drawn rather crudely from raw T_1 data. Comparisons can also be made to bulk polymer data. Figure 10 shows temperature-dependent ^{13}C NMR spin-lattice relaxation times for neat Aroclor, bulk polybutadiene, and polybutadiene in dilute polybutadiene/Aroclor solutions. The curves through the Aroclor and dilute solution polybutadiene data are the best fits calculated above. The bulk polybutadiene data are from ref 21 and have been transposed to a Larmor frequency of 90.6 MHz according to the method presented in that paper. Linear segments connecting these points are included to help guide the eye.

The prominent feature of Figure 10 is the existence of a minimum T_1 for each of the three curves. These minima result from a resonance between the Larmor frequency and a time scale τ for molecular motion. As a crude approximation, the minima occur when $\omega\tau \approx 1$. $\tau_{\text{Aro}} \approx 2$ ns at 303 K in neat Aroclor, $\tau_{\text{PB}} \approx 2$ ns at 286 K for a dilute solution of polybutadiene in Aroclor, and $\tau_{\text{PB}} \approx 2$ ns at 269 K in bulk polybutadiene. All of these time constants decrease at higher temperature.

Normally the molecular mobility of a small-molecule liquid is much greater than the local mobility of a bulk polymer. Therefore, the T_1 minimum of the small molecule usually occurs at a much lower temperature than that for the polymer. For example, the T_1 minimum for polystyrene occurs at about 450 K,^{42–45} whereas the minimum for Aroclor is at 303 K. Numerous other examples with more common solvents are available. The situation for Aroclor and polybutadiene, depicted in Figure 10, is a rare counterexample. The T_1 minimum for bulk polybutadiene occurs at a temperature 34 K cooler than for neat Aroclor. Therefore, the microscopic mobility of polybutadiene in the bulk is greater than that of neat Aroclor.

Normally when a small-molecule liquid is added to a polymer, the small molecule plasticizes the polymer. Polymer motions in the mixture become faster than those in the undiluted polymer. Therefore, the polymer T_1 minimum normally occurs at lower temperature in dilute

solutions than in bulk polymer. Indeed this is the case for nearly all polymer/solvent systems, presumably including polystyrene/Aroclor. The situation for polybutadiene/Aroclor, shown in Figure 10, again is just the opposite. Polybutadiene local motions are faster in bulk polybutadiene than in dilute solutions with Aroclor.

Morris, Amelar, and Lodge considered free volume and macroscopic plasticization effects in polymer/Aroclor mixtures.⁶ Although such arguments predicted some features of their data, important qualitative discrepancies remained. In particular, the temperature variations of $\partial \ln \zeta(c, T) / \partial c$ for the different polymer/Aroclor solutions could not be reconciled. As noted by these authors, free volume concepts are difficult to quantify at a molecular level. The times required for solvent motions and polymer dynamics on the length scale of a solvent molecule can be interpreted as microscopic indications of the available free volume. Hence, our comparison of local polymer and solvent mobilities can be considered a microscopic extension of the macroscopic plasticization argument presented by Morris et al.

Solvents Other Than Aroclor. In Aroclor solutions the modifications of the solvent dynamics are fundamentally related to the time scales for local polymer motions. The pertinent polymer motions occur on a length scale approximately equal to the size of a solvent molecule. When these motions are slower than Aroclor rotational dynamics, solvent rotation becomes slower as the polymer concentration increases. Likewise, when local polymer dynamics are faster than solvent rotational dynamics, solvent rotation is facilitated by addition of polymer. The conclusions from Figure 9 can be cast in equation form

$$\frac{\partial}{\partial c} \ln \left(\frac{\tau_{\text{solv}}(c, T)}{\tau_{\text{solv}}} \right) \approx Q \log \left(\frac{\tau_{\text{poly}}}{\tau_{\text{solv}}} \right) \quad (17)$$

where $\tau_{\text{solv}}(c, T)$ is a time constant characterizing solvent motions and $\tau_{\text{solv}} \equiv \tau_{\text{solv}}(0, T)$. For the solvent Aroclor 1248, $Q \approx 4 \text{ mL/g}$.

Important questions of generality remain. What happens to solvent rotations in other polymer solutions? Can the relative time scales for polymer and solvent dynamics predict the behavior of other solvents? These questions cannot be entirely answered at present. Local segmental dynamics are as fast or faster than solvent rotations in some other systems: polyisoprene/squalane,¹³ polybutadiene/squalene⁴⁶ and polybutadiene/bis(2-ethylhexyl) phthalate.⁴⁶ We anticipate that $\partial \ln \zeta(c, T) / \partial c < 0$ and perhaps that $(\eta_{\infty}' - \eta_s) < 0$ for these solutions.

Some information is available concerning solvent modification effects for solvents other than Aroclor. Solvent rotation times have been measured for polystyrene solutions in toluene and tetrahydrofuran. If eq 17 can explain the dynamics of these systems, Q must be different for different solvents. In polystyrene/toluene, depolarized Rayleigh line widths indicate $\partial \ln \zeta(c, T) / \partial c \approx 0.8 \text{ mL/g}$.⁴⁷ ²H NMR T_1 s of polystyrene/toluene- d_8 suggest $\partial \ln \zeta(c, T) / \partial c \approx 3 \text{ mL/g}$.⁴⁸ Both sets of experiments were performed near room temperature. As these values are both rather small, comparisons to Figure 9 or eq 17 suggest that $\log(\tau_{\text{PS}}/\tau_{\text{toluene}}) < 0.8$. However, ¹³C NMR T_1 s demonstrate otherwise. $T_1 \geq 15 \text{ s}$ for neat toluene,⁴⁹ and $T_1 \approx 0.1 \text{ s}$ for dilute polystyrene (backbone C-H) in toluene.³⁴ Since T_1^{-1} is approximately proportional to τ , $\log(\tau_{\text{PS}}/\tau_{\text{toluene}}) \geq 2.2$. Therefore, if the discussion regarding Figure 9 and eq 17 is valid for polystyrene/toluene mixtures also, $Q_{\text{toluene}} < 1.4 \text{ mL/g}$, significantly smaller than $Q_{\text{Aro}} \approx 4 \text{ mL/g}$. In a similar manner, NMR

T_1 s at 298 K demonstrate that for polystyrene/tetrahydrofuran, $Q_{\text{THF}} \leq 0.5 \text{ mL/g}$.⁴⁶

It is not clear why solvent modification effects are so dramatic (large Q) for Aroclor solutions but not for other solvents (small Q). Q can be viewed as a parameter which indicates the coupling strength between solvent reorientation and local polymer dynamics. It may be that the size and shape of the solvent molecules are important variables. Small or nearly spherical molecules may be less affected by the presence of a nearby polymer chain. Lodge and co-workers suggest that orientational ordering of many Aroclor molecules could facilitate strong coupling between solvent and polymer motions.⁷ This question may be suited to analysis by the coupling model.⁹

Summary

Dynamic mechanical measurements of polymer solutions show anomalous behavior at high frequencies. Lodge and co-workers have demonstrated that these effects are due to modifications of the solvent dynamics due to the presence of the polymer. We have extended their work through ¹³C NMR relaxation experiments. This technique allows us to monitor simultaneously the rotational dynamics of the solvent (Aroclor 1248) and the local conformational dynamics of the polymer.

Differences in time scale between local polymer and Aroclor motions are strongly correlated with the changes in Aroclor relaxation times as the polymer concentrations increase. In polystyrene/Aroclor solutions, local polymer dynamics are slower than neat Aroclor motions, so Aroclor dynamics become slower in more concentrated solutions. In polybutadiene and polyisoprene solutions, polymer motions are faster than those of Aroclor and Aroclor motions become faster in more concentrated solutions. All of these changes have been addressed quantitatively. For the three polymer/Aroclor solutions, the relative time scales for polymer and solvent dynamics account for the directions of the modifications to Aroclor dynamics, the relative magnitudes of these changes, and their different temperature dependences.

Acknowledgment. This research was supported by the National Science Foundation (Division of Materials Research, Polymers Program, Grant 8822076). D.J.G. is grateful for fellowship support from IBM. M.D.E. thanks the Alfred P. Sloan Foundation for fellowship support. NMR experiments were performed in the Instrument Center of the Department of Chemistry, University of Wisconsin. We thank the staff for assistance. We have benefitted greatly from discussions with Tim Lodge and John Schrag. In addition we thank Tim Lodge, G. Fytas, Franz Fajara, and their co-workers for allowing us to include unpublished results.

References and Notes

- (1) Ferry, J. D. *Viscoelastic Properties of Polymers*; John Wiley & Sons: New York, 1980; Chapter 9.
- (2) Merchak, P. A. Ph.D. Thesis, University of Wisconsin, 1987.
- (3) Stokich, T. M. Ph.D. Thesis, University of Wisconsin, 1988.
- (4) Strand, D. A. Ph.D. Thesis, University of Wisconsin, 1989.
- (5) Bird, R. B. *Rheol. Acta* 1989, 28, 457.
- (6) Morris, R. L.; Amelar, S.; Lodge, T. P. *J. Chem. Phys.* 1988, 89, 6523.
- (7) Amelar, S.; Krahn, J. R.; Hermann, K. C.; Morris, R. L.; Lodge, T. P. *Spectrochim. Acta Rev.*, in press.
- (8) Fixman, M. *J. Chem. Phys.* 1990, 92, 6858.
- (9) Ngai, K. L. *J. Polym. Sci., Polym. Phys. Ed.* 1991, 29, 867.
- (10) von Meerwall, E. D.; Amelar, S.; Smeltzly, M. A.; Lodge, T. P. *Macromolecules* 1989, 22, 295.
- (11) Fytas, F.; Rizos, A.; Floudas, G.; Lodge, T. P. *J. Chem. Phys.* 1990, 93, 5096.

- (12) Rizos, A.; Fytas, G.; Lodge, T. P.; Ngai, K. L. *J. Chem. Phys.* **1991**, *95*, 2980.
- (13) Glowinkowski, S.; Gisser, D. J.; Ediger, M. D. *Macromolecules* **1990**, *23*, 3520.
- (14) Gisser, D. J.; Glowinkowski, S.; Ediger, M. D. *Macromolecules* **1991**, *24*, 4270.
- (15) Harris, J. S. *Prod. Eng.* **1954**, *25* (December), 163.
- (16) See, for example: Bovey, F. A. *Nuclear Magnetic Resonance Spectroscopy*, 2nd ed.; Academic Press: San Diego, CA, 1988; Chapter 5.
- (17) *Sadtler Standard Carbon-13 NMR Spectra*; Sadtler Research Laboratories: Philadelphia, PA, 1976.
- (18) Duch, M. W.; Grant, D. M. *Macromolecules* **1970**, *3*, 165.
- (19) Lyerla, J. R.; Levy, G. C. *Top. Carbon-13 NMR Spectrosc.* **1974**, *1*, 79.
- (20) See: Reference 16, p 404.
- (21) Guillermo, A.; Dupeyre, R.; Cohen-Addad, J. P. *Macromolecules* **1990**, *23*, 1291.
- (22) A notational error in endnote 25 of ref 14 incorrectly defines $\phi = \omega_0^2 T_1^{\text{dd}} / T_1^{\text{CSA}}$. The correct definition is $\phi = T_1^{\text{dd}} / \omega_C^2 T_1^{\text{CSA}}$.
- (23) Heatley, F. *Prog. Nucl. Magn. Reson. Spectrosc.* **1979**, *13*, 47.
- (24) Cole, K. S.; Cole, R. H. *J. Chem. Phys.* **1941**, *9*, 341.
- (25) Fuoss, R. M.; Kirkwood, J. G. *J. Am. Chem. Soc.* **1941**, *63*, 385.
- (26) Schaefer, J. *Macromolecules* **1973**, *6*, 882.
- (27) Gotlieb, Yu. Ya.; Neyelov, I. M.; Torchinskii, I. A. *Polym. Sci. USSR* **1989**, *31*, 1976.
- (28) Davidson, D. W.; Cole, R. H. *J. Chem. Phys.* **1950**, *18*, 1417.
- (29) Reference 11 shows that small deviations from eq 7 may exist for neat Aroclor. These deviations are too small to affect substantially any conclusions presented in this paper.
- (30) Adolf, D. B.; Ediger, M. D. *Macromolecules* **1991**, *24*, 5834.
- (31) Adolf, D. B.; Ediger, M. D.; Kitano, T.; Ito, K. *Macromolecules*, in press.
- (32) Inoue, Y.; Konno, T. *Polym. J.* **1976**, *8*, 457.
- (33) Gronski, W.; Murayama, N. *Makromol. Chem.* **1978**, *179*, 1509.
- (34) Gronski, W.; Schäfer, T.; Peter, R. *Polym. Bull.* **1979**, *1*, 319.
- (35) Heatley, F.; Wood, B. *Polymer* **1978**, *19*, 1405.
- (36) Grandjean, J.; Sillescu, H.; Willenberg, B. *Makromol. Chem.* **1977**, *178*, 1445.
- (37) Waldow, D. A.; Ediger, M. D.; Yamaguchi, Y.; Matsushita, Y.; Noda, I. *Macromolecules* **1991**, *24*, 3147.
- (38) Grote, R. F.; Hynes, J. T. *J. Chem. Phys.* **1980**, *73*, 2715.
- (39) Bagchi, B.; Oxtoby, D. W. *J. Chem. Phys.* **1983**, *78*, 2735.
- (40) Flom, S. R.; Nagarajan, V.; Barbara, P. F. *J. Phys. Chem.* **1986**, *90*, 2092.
- (41) Brearly, A. M.; Flom, S. R.; Nagarajan, V.; Barbara, P. F. *J. Phys. Chem.* **1986**, *90*, 2092.
- (42) To our knowledge, the ^{13}C T_1 minimum has not been measured for polystyrene melts. For other polymers the minimum occurs at about $T_g + 80$ K. Several studies of polystyrene ^1H T_1 s have been reported.⁴³⁻⁴⁵ At $\omega_H = 90$ MHz the ^1H T_1 minimum is ~ 475 K.
- (43) Froix, M. F.; Williams, D. J.; Goedde, A. O. *Macromolecules* **1976**, *9*, 354.
- (44) Lindner, P.; Rössler, E.; Sillescu, H. *Makromol. Chem.* **1981**, *182*, 3653.
- (45) Schnur, G.; Kimmich, R. *Chem. Phys. Lett.* **1988**, *144*, 333.
- (46) Gisser, D. J.; Ediger, M. D., to be published in *Macromolecules*.
- (47) Patterson, G. D.; Lindsey, C. P.; Alms, G. R. *Macromolecules* **1978**, *11*, 1242.
- (48) Fujara, F.; Sillescu, H.; Lodge, T. P., unpublished results.
- (49) Levy, G. C. *J. Chem. Soc., Chem. Commun.* **1972**, 47.